

High degree of current rectification at nanoscale level

Madhumita Saha¹ and Santanu K. Maiti^{1,*}

¹*Physics and Applied Mathematics Unit, Indian Statistical Institute,
203 Barrackpore Trunk Road, Kolkata-700 108, India*

We address an unexpectedly large rectification using a simple quantum wire with correlated site potentials. The external electric field, associated with voltage bias, leads to unequal charge currents for two different polarities of external bias and this effect is further enhanced by incorporating the asymmetry in wire-to-electrode coupling. Our calculations suggest that in some cases almost cent percent rectification is obtained for a wide bias window. This performance is valid against disorder configurations and thus we can expect an experimental verification of our theoretical analysis in near future.

I. INTRODUCTION

Designing of an efficient rectifier at nanoscale level has been the subject of intense research after the prediction of molecular rectifier by Aviram and Ratner¹ in 1974. Following this pioneering work, interest in this area has rapidly picked up with several theoretical propositions and experimental verifications and most of these works involve small organic molecules with donor-acceptor pair between metallic electrodes²⁻¹³. Recently a DNA-based rectifier has also been established¹⁴ which exhibits a large rectification ratio of about 15 at 1.1 V.

To achieve rectification (viz, $I(V) \neq I(-V)$), energy levels of the bridging material have to be aligned differently for the positive and negative biases. This can

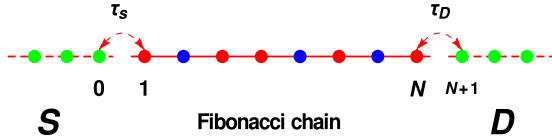


FIG. 1: (Color online). Quasi-periodic (Fibonacci, 5th generation i.e., 8 atomic sites) chain attached to 1D source (S) and drain (D) electrodes. The filled red and blue circles correspond to two different lattices (say) A and B , respectively.

be done in two different ways: (i) placing an asymmetric conductor between source and drain electrodes^{10,12}, keeping identical conductor-to-electrode couplings, and (ii) considering a symmetric conductor with unequal conductor-electrode couplings¹³. The understanding is that for both these two cases resonant energy levels, in presence of finite bias, are arranged distinctly for two different biased conditions which results finite rectification. Therefore, when both these two conditions are satisfied one can expect maximum rectification.

So far mostly molecular systems⁷⁻¹³ have been used to design rectifying diodes, but constructing them using single molecules is a major challenge¹⁵ and still many open questions remain which certainly demand further study. Therefore, *designing of a rectifier using simple geometric structure which provides high rectification ratio is a matter of great interest*. In the present work we essentially focus on it and make an attempt to es-

tablish that a simple 1D chain with correlated site potentials can exhibit a very high degree of rectification, and sometimes it becomes nearly close to $\pm 100\%$ for a wide bias window. This performance is valid against disordered configurations which we confirm by comparing the results of different 1D quasi-periodic chains like Fibonacci (Fibo), Thou-Morse (TM), Copper-mean (CM) and Bronze-mean (BM) and all these systems are constructed by using two primary lattices, namely A and B , following the specific inflation rules¹⁶⁻¹⁸. For the case of Fibonacci chain the rule is: $A \rightarrow AB$ and $B \rightarrow A$. Therefore, applying successively this substitutional rule, starting with A or B lattice we can construct the full lattice chain for any particular generation, say p -th generation, obeying the prescription $F_p = F_{p-1} \otimes F_{p-2}$. So, if we start with A lattice then the first few generations of the Fibonacci series are $A, AB, ABA, ABAAB, ABAABABA, \dots$, etc. The inflation rules for the other three quasiperiodic chains which we consider here i.e., TM, CM and BM are: $A \rightarrow AB, B \rightarrow BA$; $A \rightarrow ABB, B \rightarrow A$, and $A \rightarrow AAAB, B \rightarrow A$, respectively. Using these rules we construct the quasiperiodic chains for any desired generation starting with any lattice site A or B .

The rest of the paper is arranged as follows. In Sec. II we present the model and theoretical framework for calculations. The results are described in Sec. III, and finally, in Sec. IV we conclude our findings.

II. MODEL AND THEORETICAL FRAMEWORK

The calculations are worked out using wave-guide theory based on tight-binding (TB) framework. In this framework the Hamiltonian of the full system, schematically shown in Fig. 1, can be written as $H = H_{el} + H_{ch} + H_{tn}$, where H_{el} , H_{ch} and H_{tn} correspond to the Hamiltonians of the electrodes (source and drain), quasi-periodic chain and chain-to-electrode tunneling coupling, respectively. In terms of on-site potential ϵ_i and nearest-neighbor hopping integral t , the TB Hamiltonian of the chain can be written as:

$$H_{ch} = \sum_{i=1} \epsilon_i c_i^\dagger c_i + \sum_{i=1} t \left(c_{i+1}^\dagger c_i + c_i^\dagger c_{i+1} \right) \quad (1)$$

where c_i^\dagger (c_i) represents the electronic creation (annihilation) operator.

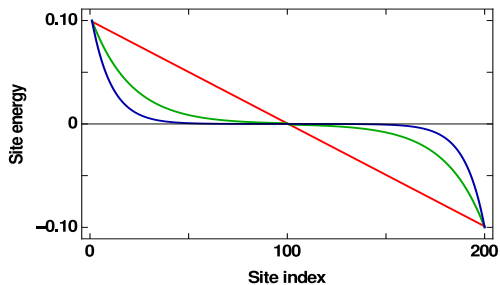


FIG. 2: (Color online). Voltage dependent site energies of a 200-site chain for three different electrostatic potential profiles, shown by three distinct colored curves, at the bias voltage $V = 0.2$ V.

operator. In a similar way we can write the TB Hamiltonian H_{el} of the two side-attached perfect 1D electrodes parameterized by ϵ_0 and t_0 . These electrodes are coupled to the sites 1 and N of the conductor (described by H_{tn}) through the coupling parameters τ_S and τ_D (see Fig. 1), where N being the total number of lattice sites of the bridging conductor.

In presence of a finite bias V between the source and drain, an electric field is developed across the chain and hence its site energies are voltage dependent^{19,20}. It gives $\epsilon_i = \epsilon_i^0 + \epsilon_i(V)$, where ϵ_i^0 is voltage independent and it becomes ϵ_A or ϵ_B depending on the lattice sites A or B . The dependence of $\epsilon_i(V)$ is associated with electron screening as well as bare electric field at the junction. In the absence of any screening electric field is uniform across the junction^{19,20} which makes $\epsilon_i(V) = V/2 - iV/(N+1)$ (linear variation, red line of Fig. 2) for a N -site chain. Whereas, long-range electron screening makes the profile non-linear as shown by the green and blue curves of Fig. 2. In our calculations we consider these three different potential profiles to have a complete idea about the bare and the screened electric field profiles, and their effects on rectification as in realistic case different materials possess different electron screening which will yield different field variations. For a slight variation from these potential profiles no significant change is observed in the physical properties, and thus our findings may be implemented in realistic cases.

To evaluate transmission probability across the conducting junction we solve a set of coupled linear equations containing wave amplitudes of distinct lattice sites of the chain^{21,22}. Assuming a plane wave incidence, we can write the wave amplitude at any site n of the source as $A_n = e^{ikn} + re^{-ikn}$, where k is the wave-vector and r being the reflection coefficient. While, for the drain electrode we get $B_n = \tau e^{ikn}$, where τ represents the transmission coefficient. For each k , associated with the injecting electron energy, we find the transmission probability from the expression $T(E) = |B_1|^2 = |\tau|^2$. Once it is determined, the net junction current for a particular bias voltage V at absolute zero temperature is obtained

from the relation²³

$$I(V) = \frac{e}{\pi\hbar} \int_{E_F - \frac{eV}{2}}^{E_F + \frac{eV}{2}} T(E) dE \quad (2)$$

where E_F represents the Fermi energy. Finally, we define the rectification ratio as¹⁴ $RR = |I(V)|/|I(-V)|$. $RR = 1$ suggests no rectification. In all calculations we set the common parameter values as: $t = 1$ eV, $\epsilon_0 = 0$, $t_0 = 3$ eV and, unless otherwise stated $E_F = 0$.

III. RESULTS AND DISCUSSION

Now we present our results. In Fig. 3 we show the variations of $|I|$ both for the forward and reverse biased

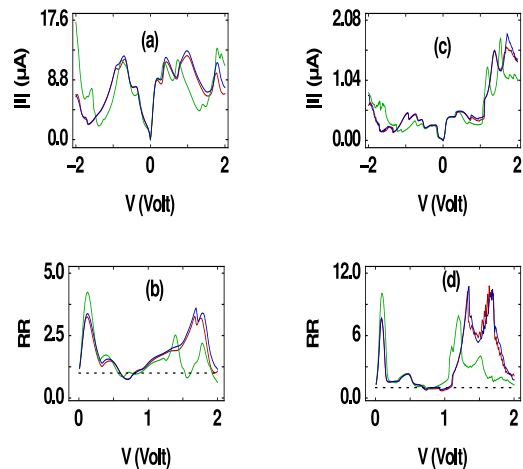


FIG. 3: (Color online). $|I|$ and RR as a function of voltage for a 8th generation ($N = 34$) Fibonacci chain with $-\epsilon_A = \epsilon_B = 0.5$ eV considering both linear (red curve) and two non-linear (green and blue curves) potential profiles. In the first column the results are shown for the symmetric coupling ($\tau_S = \tau_D = 1$ eV), while in the second column they are presented for the asymmetric coupling ($\tau_S = 0.1$ eV and $\tau_D = 1$ eV). Dashed line corresponds to $RR = 1$.

conditions along with the rectification ratio RR considering three different electrostatic potential profiles where the first and second columns correspond to the symmetric and asymmetric wire-to-electrode couplings, respectively. Two observations are noteworthy. First, the currents for the positive and negative biases are quite close to each other in the limit of symmetric coupling (Fig. 3(a)), whereas they differ distinctly in the case of asymmetric coupling (Fig. 3(c)) though the currents in this case are much less than the previous one. Second, for a wide bias window (~ 1 -2 V) the rectification ratio is significantly large, in the limit of asymmetric coupling, reaching a maximum of ~ 11 . This is a reasonably large value compared to the reported results for different conducting

junctions considering both symmetric molecular structures as well as asymmetric molecule-to-lead couplings where RR varies between 2 to $10^{10,13}$.

To illustrate the mechanism of rectification let us focus on the spectra given in Fig. 4. For the fully perfect chain ($\epsilon_i^0 = 0 \forall i$), T - E spectrum in presence of positive bias (red curve of Fig. 4(a)) exactly matches with what we get in the case of negative bias (red curve of Fig. 4(b)).

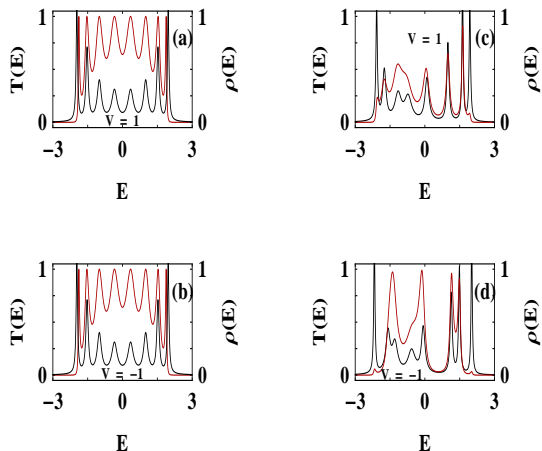


FIG. 4: (Color online). Transmission probability $T(E)$ (red color) as a function of energy E for ordered ($\epsilon_i = 0 \forall i$) and Fibonacci chains ($-\epsilon_A = \epsilon_B = 0.5$ eV) considering a linear bias drop. The average density of states $\rho(E)$ (black color) is superimposed in each spectrum. Here we set $\tau_S = \tau_D = 1$ eV and $N = 8$.

Therefore, for this junction identical currents are obtained upon the integration of the transmission function T , resulting a vanishing rectification. While, comparing the spectra given in Figs. 4(c) and (d), worked out for the positive and negative biases considering a Fibonacci chain, it is clearly seen that the transmission spectra differ sharply which results a finite rectification. To achieve rectification the essential thing is that, as stated earlier, the energy levels of the bridging material have to be aligned differently for the positive and negative biases. The alignments of energy levels for the two different wires are clearly reflected from the ρ - E spectra (black curves of Fig. 4). Thus increasing the misalignment higher RR is expected and it can be done further by including additional asymmetric factors like asymmetric environmental effects²⁴, inconsistent gating²⁵, etc.

Figure 5 shows the percentage of rectification (defined as $(|I(V)| - |I(-V)|)/(|I(V)| + |I(-V)|) = (RR - 1)/(RR + 1)$) as a function of voltage for three different sizes of the Fibonacci chain. Quite interestingly we see that for *wide voltage regions nearly cent percent rectification is obtained*, and thus the present system can be utilized as a perfect rectifier.

In order to justify the robustness of rectification against disorderness, in Fig. 6 we present RR - V characteristics for some typical quasi-periodic lattices. All these

junctions provide finite rectification where RR varies in a wide range, and from these curves it can be emphasized that any one of such lattices can be used to achieve the

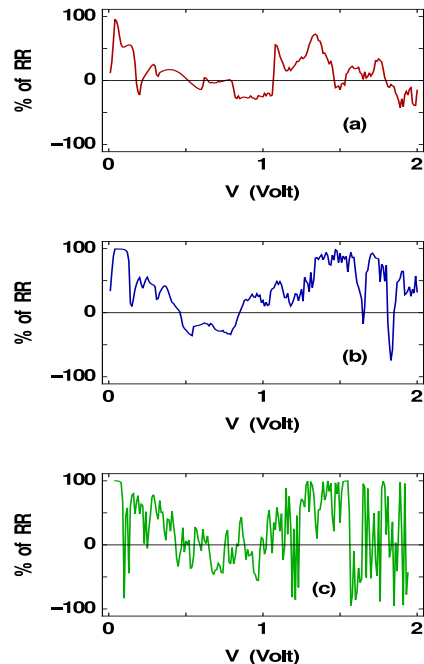


FIG. 5: (Color online). Percentage of RR as a function of bias voltage V for three different sizes of the Fibonacci chain considering a linear bias drop, where (a), (b) and (c) correspond to $N = 55, 89, 233$, respectively. Here we choose $\tau_S = 0.1$ eV and $\tau_D = 1$ eV, and $-\epsilon_A = \epsilon_B = 0.5$ eV.

goal of rectification action. Looking carefully into the spectrum (Fig. 6) it is observed that RR reaches to zero ($\sim -100\%$) for a reasonable voltage window (~ 0.23 -

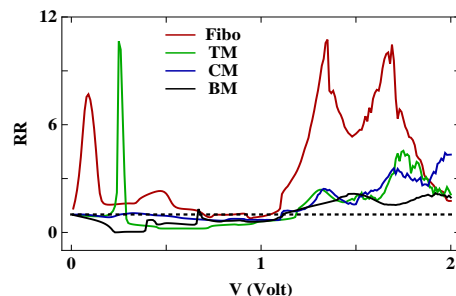


FIG. 6: (Color online). RR - V characteristics for four different quasi-periodic chains with inconsistent wire-to-electrode coupling ($\tau_S = 0.1$ eV and $\tau_D = 1$ eV) in presence of linear potential profile. Here we set $N = 34, 32, 43$ and 43 for Fibo, TM, CU and BM chains, respectively, and choose $-\epsilon_A = \epsilon_B = 0.5$ eV.

0.38 V) for the junction containing BM wire. One could also get opposite scenario i.e., $\sim +100\%$ rectification through any one of these junctions. This is solely associated with the interplay between the arrangements of

lattice sites and electrostatic potential profile.

Finally, in Fig. 7 we discuss the possibilities of regulating the rectification ratio *externally* for a fixed bias voltage. This can be achieved by tuning the Fermi en-

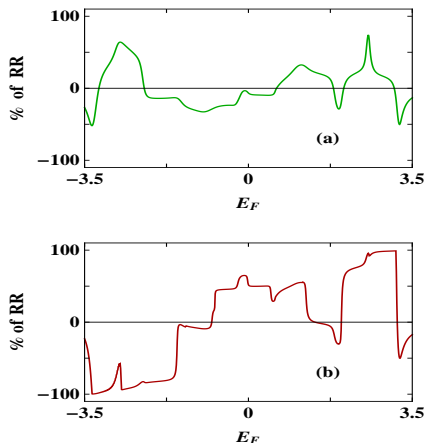


FIG. 7: (Color online). Percentage of RR as a function of Fermi energy E_F for a 5th generation Fibonacci chain ($-\epsilon_A = \epsilon_B = 0.5$ eV) considering a linear bias drop at $V = 2$ V, where (a) and (b) correspond to the symmetric ($\tau_S = \tau_D = 1$ eV) and asymmetric ($\tau_S = 0.1$ eV and $\tau_D = 1$ eV) wire-to-electrode couplings, respectively.

ergy, which on the other hand is controlled by external gate voltage. It is worthy to note that upon changing E_F one can get a wide variation of RR (viz, -100% to $+100\%$), and thus it can be emphasized that the present model can be utilized to get *externally controlled* rectifier at nano-scale level.

Before the end, we would like to point out that, apart from rectifying action all these quantum wires character-

ized by quasi-periodic lattices show another uncommon property of junction current where an increase in the bias voltage results a reduction of net current (see Figs. 3 and 6). This is the so-called negative differential conductance (NDC) effect²⁶, and its detailed analysis will be given in our forthcoming paper.

IV. CONCLUDING REMARKS

To conclude, in the present work we have attempted to establish a model quantum system that can exhibit a high degree of current rectification at nanoscale level. An unexpectedly large rectification ratio has been obtained, and most importantly, we see that in some cases nearly cent percent rectification can be achieved for a wide bias window. Our results are also valid against disordered configurations which we have confirmed by considering different kinds of disordered systems. Though the proposition given here is based on purely theoretical arguments, we hope that its experimental verification can be done in near future.

Finally, we want to note that although the results have been worked out at zero temperature, all the physical features remain invariant at finite temperature (~ 300 K) as thermal broadening of energy levels is much weaker than the broadening caused as a result of wire-to-electrode couplings²³.

V. ACKNOWLEDGMENT

MS would like to acknowledge University Grants Commission (UGC) of India for her research fellowship.

* Electronic address: santanu.maiti@isical.ac.in

¹ A. Aviram and M. A. Ratner, Chem. Phys. Lett. **29**, 277 (1974).
² A. Dhirani, P. -H. Lin, P. Guyot-Sionnest, R. W. Zehner, and L. R. Sita, J. Chem. Phys. **106**, 5249 (1997).
³ C. Zhou, M. R. Deshpande, M. A. Reed, L. Jones II, and J. M. Tour, Appl. Phys. Lett. **71**, 611 (1997).
⁴ J. Frantti, V. Lantto, S. Nishio, and M. Kakihana, Phys. Rev. B **59**, 12 (1999).
⁵ R. M. Metzger, Acc. Chem. Res. **32**, 950 (1999).
⁶ J. Taylor, M. Brandbyge, and K. Stokbro, Phys. Rev. Lett. **89**, 138301 (2002).
⁷ G. J. Ashwell, W. D. Tyrrell, and A. J. Whittam, J. Am. Chem. Soc. **126**, 7102 (2004).
⁸ I. Díez-Pérez *et al.*, Nature Chem. **1**, 635 (2009).
⁹ C. A. Nijhuis, W. F. Reus, and G. M. Whitesides, J. Am. Chem. Soc. **132**, 18386 (2010).
¹⁰ S. K. Yee *et al.*, ACS Nano **5**, 9256 (2011).
¹¹ A. Batra *et al.*, Nano Lett. **13**, 6233 (2013).
¹² H. J. Yoon *et al.*, J. Am. Chem. Soc. **136**, 17155 (2014).
¹³ K. Wang, J. Zhou, J. M. Hamill, and B. Xu, J. Chem.

Phys. **141**, 054712 (2014).
¹⁴ C. Guo *et al.*, Nature Chem. **8**, 484 (2016).
¹⁵ D. Janes, Nature Chem. **1**, 601 (2009).
¹⁶ A. M. Guo, Phys. Rev. E **75**, 061915 (2007).
¹⁷ H. Lei, J. Chen, G. Nouet, S. Feng, Q. Gong, and X. Jiang, Phys. Rev. B **75**, 205109 (2007).
¹⁸ M. Patra and S. K. Maiti, Ann. Phys. **375**, 337 (2016).
¹⁹ S. Pleutin, H. Grabert, G. L. Ingold, and A. Nitzan, J. Chem. Phys. **118**, 3756 (2003).
²⁰ S. K. Maiti and A. Nitzan, Phys. Lett. A **377**, 1205 (2013).
²¹ Y. J. Xiong and X. T. Liang, Phys. Lett. A **330**, 307 (2004).
²² M. Patra and S. K. Maiti, Sci. Rep. **7**, 43343 (2017).
²³ Datta, S. Electronic transport in mesoscopic systems. Cambridge University Press, Cambridge (1997).
²⁴ B. Capozzi *et al.*, Nature Nanotech. **10**, 522 (2015).
²⁵ B. Capozzi *et al.*, Nano Lett. **14**, 1400 (2014).
²⁶ B. Xu and Y. Dubi, J. Phys.: Condens. Matter **27**, 263202 (2015).